

MEASUREMENT OF THE AERODYNAMICS IN THE PRIMARY ZONE OF A LOW-NO_x COMBUSTOR AT ATMOSPHERIC AND ISOTHERMAL CONDITIONS

Christian Faustmann

Graz University of Technology
Institute for Thermal Turbomachinery and
Machine Dynamics
Inffeldgasse 25A, 8010 Graz - Austria

Andreas Lang

Andritz Hydro GmbH
Dr. Karl-Widdmann-Straße 5, 8160 Weiz - Austria

Fabrice Giuliani

Combustion Bay One
Science Park Graz
Plüddemanngasse 39, 8010 Graz - Austria

ABSTRACT

The present paper would complete a lack of information on the aerodynamics of low-NO_x combustors. The Lean-Premixed-Prevapourized (LPP) technology is theoretically well described, but not a lot of experimental results can be found in literature. In the present paper Laser Doppler Anemometry (LDA) measurements in a test rig modelling a sector of annular reverse flow type combustor chamber are presented. The facility consists of an assembly with two liquid fuelled, low-NO_x industrial burners as well as a pilot burner. Each burner is separately fed. Three optical accesses allow the use of non-intrusive optical measurement techniques for a description of the primary combustor zone. This contribution refers to the preliminary characterization of the test section, which was already investigated at Graz University of Technology (TU Graz). Experiments were performed at atmospheric conditions without combustion in order to determine the flow dynamics inside the test section. Using a multi component LDA system in two perpendicular directions, the three dimensional flow field, consisting of the coincident mean velocities including most of the Reynolds stresses, was measured. The results show good agreement with what can be found in literature on the LPP technology, in particular no recirculation zone was found and the mean swirl number of $S=0.32$ is also lower than the critical swirl number of 0.4.

INTRODUCTION

In the next 20 years Wilfert et al. [1] forecast the expansion rate of the global air traffic with 5% per year. To handle the growth of air pollution caused by this high level of growth in the air traffic, new aero core concepts have to be developed and validated. This research takes place in the NEWAC-Project founded by the European Union under the leadership of MTU Aero Engines. The targets of NEWAC are fully validated new technologies that will reduce CO₂ emissions by 6% and NO_x by 16% [2]. The Institute of Thermal Turbomachinery and

Machine Dynamics (TTM) at TU Graz is one of 40 partners in the NEWAC-program and is participating on subproject 6 (Innovative Combustion). The investigation is focused on the stability of combustion in a test sector combustion chamber equipped with LPP-modules. The combustor is part of the Intercooled Recuperative Aero Engine (IRA) shown in figure 1 and is of the reverse flow type. The test sector under investigation is a sector of this combustor and bends into a planar shape to ease the optical accessibility.

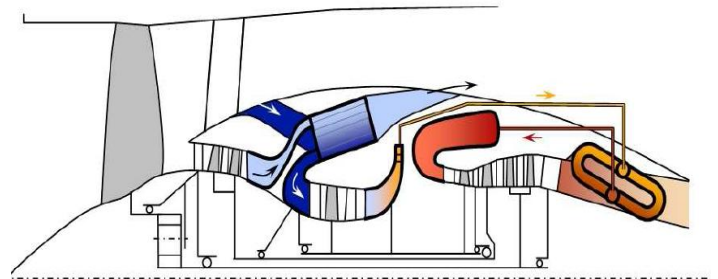


Fig. 1 Intercooled Recuperative Aero engine with NEWAC combustion chamber [1]

Limited information is available on the LPP-technology (Lean Premixed Prevapourized) in the open literature. Some basics can be found in [3]. More details on overall pressure ratio (OPR) and the risks of auto-ignition and flash-back are given in [1].

The aerodynamic phenomena of the LPP-technology were investigated at ambient conditions without any flame. Therefore a test rig was built at the TU Graz, to measure the three velocity components in different planes at the LPP-modules. A 2D-LDA-System (Laser Doppler Anemometry) was used to get 3D information of the aerodynamics in the primary Zone of a Low-NO_x-Combustor. Measuring data were processed with MathWorks MATLAB.

EXPERIMENTAL SETUP

The cold flow LDA-tests were performed on a test bench at the Institute for Thermal Turbomachinery and Machine Dynamics at TU Graz. The test rig is designed for the investigation of the cold flow at the combustor primary zone. The test rig itself consists of the following components:

- air supply
- air piping and manual pressure regulation valves
- mass flow meter
- seeding generator
- traversing system
- LDA-System

A separate air supply is used for each LPP-module. The mass flow is metered by V-Cones. The airflow was seeded with oil droplets (di-ethyl-hexyl-sebacat, DEHS), acting as a tracer for the LDA measurements. Each air supply was equipped with a dedicated seeding generator producing an aerosol with a specific particle size of $0.3\mu\text{m}$. A two component LDA (DANTEC Fiber-Flow with DANTEC Burst Spectrum Analyzer, DANTEC Dynamics, Roskilde Denmark) fed by an argon ion laser (Coherent Inc., Santa Clara, CA) with wavelengths $\lambda_{\text{laser}} = 488\text{ nm}$ and 514.5 nm was used. To obtain three dimensional information on the aerodynamics in the primary zone of each LPP-module data was acquired in three perpendicular planes as shown in Fig. 2. There the black circles represent exits of the LPP-modules and the black cube represents the combustion chamber. The x-z- and the x-y-planes are the horizontal and vertical planes located at the center of the LPP-module exits. The blue y-z-plane is located one diameter downstream of the LPP modules.

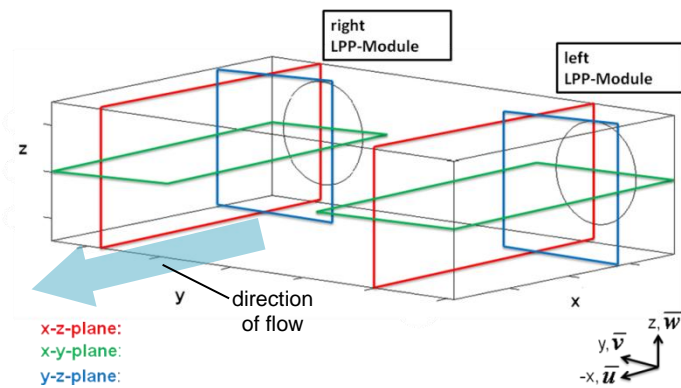


Fig. 2 Measurements planes in respect to the LPP injector exits

Due to the fact that an optical measurement technique is used, optical accessibility to the measurement volume is essential. Two windows frame the vertical sidewalls and a third window is installed at the bottom of the combustor. All windows are made of quartz glass, having a good characteristic concerning refraction of the laser beam. In addition the quartz glass is high temperature resistant, which is essential for tests

reaching realistic combustor conditions that took place in the past and can be seen in [8].

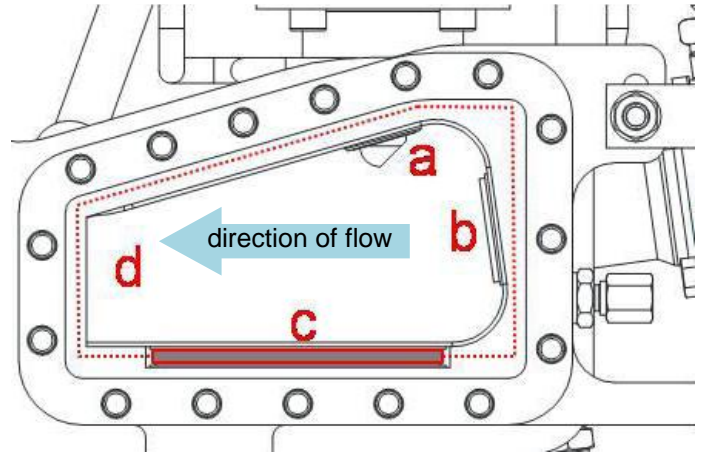


Fig. 3 Lateral view of the combustor

Fig. 3 shows the combustor in a lateral view, where label *a* shows the position of the pilot burner, *b* represents the exit of a LPP-module and the captions *c* and *d* represent the optical accesses on the side walls (dotted line) and bottom.

Besides the three optical accesses two different setups are needed to get a 3D-characteristic of the flow in the combustor with a 2D-LDA-System. Positioning of the optical head was done in both setups with a DANTEC lightweight traverse where the LDA probe was fixed perpendicular to the respective side windows and operated in backscatter mode. The two setups named A and B are shown in Figs. 4 (A) and 5 (B). For ease of operation the change between the setups is achieved by rotating the combustor by 90° such that the respective window was aligned with the LDA probe. In Fig. 4 setup A is shown where the axial and tangential component of velocity and the $\overline{u'^2}, \overline{w'^2}, \overline{u'w'}$ components of the Reynolds tensor can be measured. In Fig. 5, setup B, the axial and the radial components of velocity and the $\overline{u'^2}, \overline{v'^2}, \overline{u'v'}$ correlations are measured. To provide the data with respect to the individual LPP module axis, coordinate transformation was used. A particular problem with seeded flow is the deposition of the seeding on the windows which deteriorates the data rate. Using the DEHS seeding the problem could be overcome by heating the diagnostic window with hot air, such that the seeding evaporated keeping the windows clear.

$$\overline{u'_i u'_j} = \frac{\sum_{k=1}^N (u_{i,k} - \bar{u}_i)(u_{j,k} - \bar{u}_j) \Delta t_k}{\sum_{k=1}^N \Delta t_k} \quad \text{Eq. 3}$$

Multiplying Eq. 2 and Eq. 3 with the density will lead to the Reynolds' stress tensor. The entries on the principal diagonal are the normal stresses in the respective direction whereas the off-diagonal elements represent the shear stresses.

$$T_t = -\rho \begin{pmatrix} \overline{u'^2} & \overline{u'v'} & \overline{u'w'} \\ \overline{v'u'} & \overline{v'^2} & \overline{v'w'} \\ \overline{w'u'} & \overline{w'v'} & \overline{w'^2} \end{pmatrix} \quad \text{Eq. 4}$$

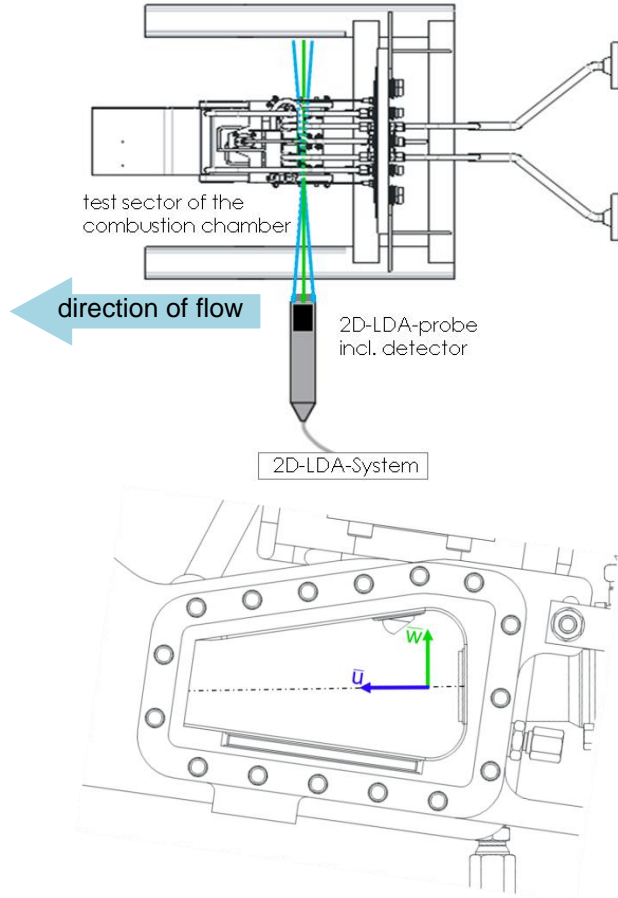


Fig. 4: Measurement setup A; top: top view of setup, bottom: measured velocities \bar{u} and \bar{w} with setup A

In addition to the three mean velocities \bar{u} , \bar{v} and \bar{w} the fluctuations of the measured data can be analyzed. Furthermore the turbulent kinetic energy and the swirl number are evaluated. Each measured data is weighted by the transit time Δt . That is the time a tracer particle needs to pass the measurement volume that is formed by the crossing laser beams [4]. For statistical analysis it is of importance to perform a weighting of the velocities with the transit time, because faster tracer particles are statistically overrepresented as slower ones. Thus weighting with the transit time comes up with a balancing of the faster and the slower tracer particles.

Eq. 1-3 show the mathematical formalism for the weighting of the mean velocity, the variance - also known as the velocity fluctuation - and the correlations of the velocity fluctuations respectively. **Table 1** shows which quantities can be computed.

$$\bar{u}_i = \frac{\sum_{k=1}^N u_{i,k} \Delta t_k}{\sum_{k=1}^N \Delta t_k} \quad \text{Eq. 1}$$

$$\overline{u_i'^2} = \frac{\sum_{k=1}^N (u_{i,k} - \bar{u}_i)^2 \Delta t_k}{\sum_{k=1}^N \Delta t_k} \quad \text{Eq. 2}$$

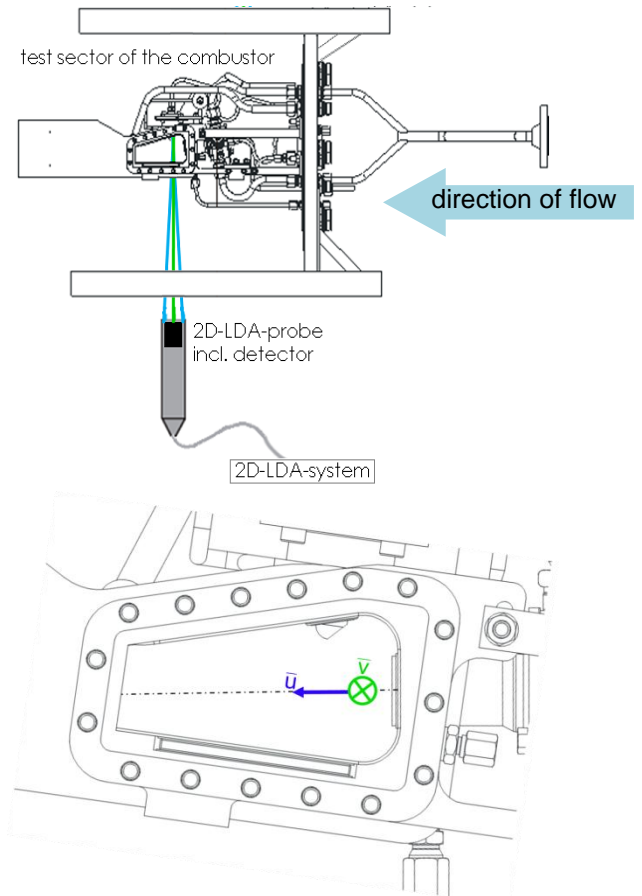


Fig. 5: Measurement setup B; top: top view of setup, bottom: measured velocities \bar{u} and \bar{v} with setup B

Furthermore for the characterization of the aerodynamics in the primary zone, the turbulent kinetic energy and the swirl number are of importance.

Assuming isentropic turbulence, Eq. 5 changes into Eq. 6. This assumption was made by reason that it is not possible to measure the diagonal elements of Eq. 4 at the same time with a two component LDA system. But one has to know that this

assumption is not valid for every measurement point in the flow field.

$$k = \frac{1}{2}(\overline{u'^2} + \overline{v'^2} + \overline{w'^2}) \quad \text{Eq. 5}$$

$$k = \frac{3}{4}(\overline{u'^2} + \overline{v'^2}) \quad \text{Eq. 6}$$

The swirl number is determined in accordance with Beer and Chigier [5] and adjusted to the present problem:

- atmospheric conditions
- rotationally symmetric
- constant density / incompressibility

The equation of Beer and Chigier will thus be turned into Eq. 7 (expression for x-y-plane).

$$S = \frac{2 \sum_0^{y_{max}} \bar{w} \bar{u} y^2 \Delta y}{D \sum_0^{y_{max}} \bar{u}^2 y \Delta y} \quad \text{Eq. 7}$$

LDA-PARAMETERS AND TEST CONDITIONS

As shown in Fig. 2 measurements were performed at three different planes per LPP-module. In each plane simultaneous recording of two velocities with a 2D-LDA-System is possible. By measuring with setup A and B a resultant vector out of the three velocity components can be computed. The record length was set to 20,000 samples or a measurement time of 100 seconds. With this setup the turbulence in respect to measurement effort is well enough determined.

The measurements of the aerodynamics in the primary zone of a Low-NO_x combustor took place at atmospheric and isothermal conditions. The operating conditions were set in accordance with Turbomeca to a reduced air flow representing *take off* conditions ($\dot{m}_{red} = 0.25 \frac{kg}{s} \frac{\sqrt{k}}{100kPa}$).

LDA-PARAMETERS		
Number of data points in plane	Averaged data rate	Analyzed quantities
x-z-plane ~180	~250Hz	$\bar{u}, \bar{w}, TKE_{uw}$ $\frac{\overline{u'^2}, \overline{w'^2}, \overline{u'w'}}{}$
x-y-plane ~210	~250Hz	$\bar{u}, \bar{v}, \bar{w}, TKE_{uv}, TKE_{uw}$ $\frac{\overline{u'^2}, \overline{v'^2}, \overline{w'^2}, \overline{u'v'}, \overline{u'w'}}{}$
y-z-plane ~150	~100Hz	$\bar{u}, \bar{v}, \bar{w}, TKE_{uv}, TKE_{uw}$ $\frac{\overline{u'^2}, \overline{v'^2}, \overline{w'^2}, \overline{u'v'}, \overline{u'w'}}{}$

Table 1 LDA-Parameters

RESULTS

All results shown are non dimensional. Velocities are divided by a reference velocity u_o (calculated with help of the continuity equation, applied at the premixing tube of the LPP module; Eq. 8 and 9). All dimensions are divided by the diameter of the premixing tube D (Eq.10)

$$u_o = \frac{4 \cdot \dot{m} \cdot R \cdot T}{p \cdot D^2 \cdot \pi} \quad \text{Eq. 8}$$

$$u = \frac{\bar{u}}{u_o} \quad \text{Eq. 9}$$

$$l = \frac{\bar{l}}{l_o} \quad \text{Eq. 10}$$

Velocity plots will be shown for both LPP-modules, the velocity fluctuations will be shown at the right LPP-module in the x-y-plane only, although **Table 1** indicates that an analysis for both LPP-modules has been performed in each plane.

Fig. 6 shows the velocity plots in the x-z-plane at the right (Fig. 6 top) and left (Fig. 6 bottom) LPP-module. The black rectangle on the right side of the figure sketches the premixing tube of a LPP-module. The liner contours are shown as solid black lines. A vector of mean velocity is plotted at each location where a measurement has been performed. To reduce measurement effort the grid is spaced fine at the combustor inlet and coarser at the outlet. For the contour plots interpolations with MATLAB's *cubic* and *v4* method were used.

Both plots in Fig. 6 show that no recirculation zone at the center axes of the burners exists. This indicates that the axial impulse in direction to the combustor exit is stronger than the static pressure inside the flow. Fig. 6 further shows an asymmetric flow field of the two LPP-modules. The fluid injected by the right LPP-module tends to flow upwards (maxima of velocity above the center axis) whereas the fluid of the left one flows downwards (maxima of velocity below the center axis). Above the centerline of the right LPP-module and below the center axis of the left LPP-module the flow is nearly axial. The same conditions can be found at the combustor exit. The flow field downstream of the injector is constantly decelerating.

Furthermore the direction of the vectors next to the edges of the combustor indicates the existence of edge vortices. Because of the outer contour of the test sector this area couldn't be measured more detailed without changing the experimental setup, so no detailed investigation of this area has been done.

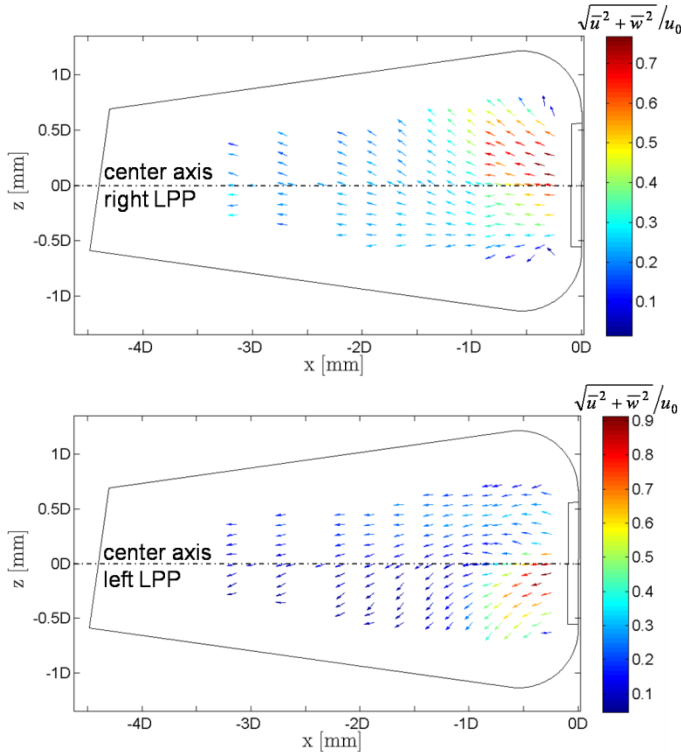


Fig. 6 Absolute velocity plots from the LDA-measurements in the x-z-plane at the right (top) and left (bottom) LPP-module

Fig. 7 shows velocity plots at the right and left LPP-module for the x-y plane. Measurements were done at the center axis ($z/D = 0$) with a radial expansion of $1D$ and nearly $3D$ in axial direction. The axial velocity u is represented by black vectors and the out of plane component w as colormap. Like in Fig. 6 the premixing tube of the LPP-modules is sketched as a black rectangle on the right side of both plots. No recirculation zone in the x-y-plane can be found. Below the center axis of the left LPP module (Fig. 7 bottom, labeled as zone 1) the flow is drastically decelerating. This can also be found, less pronounced, at the right LPP (Fig. 7 top) above its center axis. However, it can be seen when looking at cross section $x/D = -1$ that the flow field below the center axis of the left LPP is similar to the one above the center axis of the right one. The axial velocity reaches its maximum near the center of the combustor axis (LPP right: $y/D = -0.5$; LPP left: $y/D = 0.3$) and decelerates towards the combustor walls.

At both LPP-modules the out of plane velocity is in the same order of magnitude. It reaches its maximum near the outlet of the premixing tubes (located at $x/D = -0.25$, $y/D = \pm 0.5$) and slows down towards the combustor exit. This indicates a loss of angular momentum of the swirling flow. The mass flow is rotating anti clock wise at both LPP modules when looking in flow direction. Also of interest in Fig. 7 are the areas labeled with 2a and 2b. These regions are indicating a third vortex like structure existing between the two swirling flows induced by the LPP modules, which is also rotating anti clock

wise. Furthermore there must be some smaller counter rotating vortices due to the balance of angular momentum, which were not detected with this resolution of measurement points.

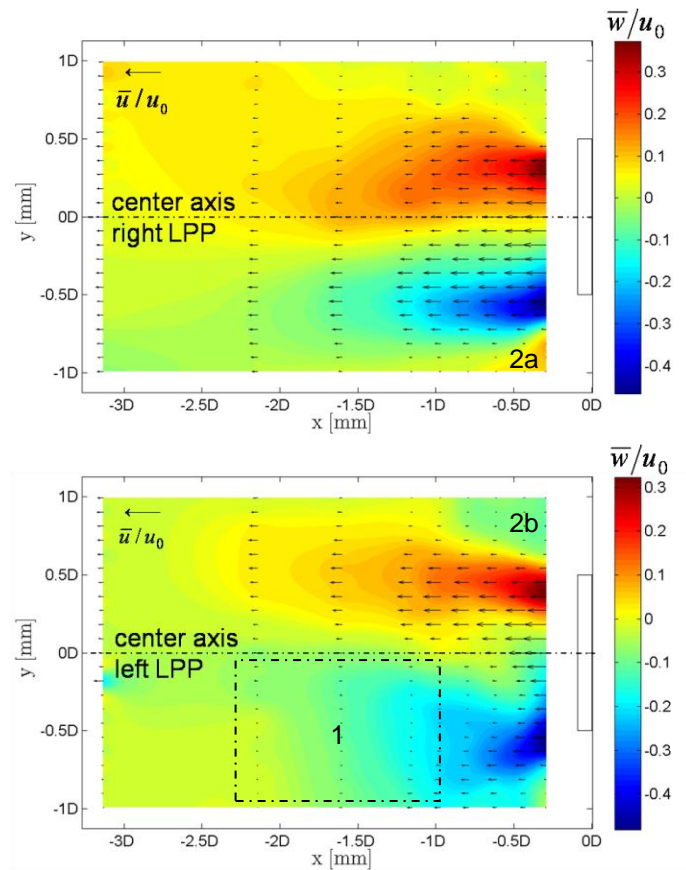


Fig. 7 Velocity plots from the LDA-measurements in the x-y-plane at the right (top) and the left (bottom) LPP-module; axial velocity shown as vectors, tangential velocity as background color

The analysis of the 2D-results is completed with the calculation of velocity fluctuations in the x-y-plane of the right LPP-module. Fig. 8a-d show beside the axial $\sqrt{u'^2}$ and tangential Root Mean Square (RMS) value $\sqrt{w'^2}$ the shear stress $\overline{u'w'}$ as well as the turbulent kinetic energy k_e .

Fig. 8 a shows that three regions of higher axial RMS values are developed at $x/D = -0.25$. A steep gradient exists at $y/D = \pm 0.5$ (labeled with 1 and 3 in Fig. 8a). The maximum of the axial RMS value is detected at the center axis next to $x/D = -0.75$ (label 2). From $x/D = -1$ to $x/D = -2$ the three regions (label 1 to 3) are forming a single large area of high level axial RMS value which is nearly expanded to the hole width of the measurement plane. Behind this line the axial RMS value decreases constantly.

Three regions of higher tangential RMS values $\sqrt{w'^2}$ are visible in Fig. 8 b). The regions are formed at the end of the

premixing tube. The fluctuation of the third velocity component has its maximum at $x/D = -0.25$, $y/D = -0.75$ and spreads up to $y/D = -2$. In comparison with $\sqrt{u'^2}$, the high level of tangential RMS values $\sqrt{w'^2}$ of the flow is centered at smaller regions. Fig. 8 c) shows the distribution of the shear stress $\overline{u'w'}$. Four areas of high level of shear stress are noticeable. The shear stress in Area 1 and 3 is negative whereas area 2 and 4 are showing a positive shear stress. The maxima are located at area 1 (positive) and 4 (negative) respectively. In these regions of high shear stress not perfectly prevaporized fuel droplets will be ruptured into smaller droplets and vaporized at high temperatures.

In the last plot of Fig. 8 the distribution of the turbulent kinetic energy k_e (TKE) is shown. Its distribution is similar to the distribution of the normal RMS values $\sqrt{u'^2}$. Three main regions with high TKE, surrounded by an intermediate level of TKE exist. The maximum itself is located at the center axis next to $x/D = -1$. Furthermore the minimum of k_e is at the same position as the minimum of both RMS values in the upper right edge of the measurement plane. In Fig. 8 d) it can be seen that the production of turbulence depends on the axial velocity component mainly and area 2 is where the biggest amount of energy dissipates.

Dividing the turbulent kinetic energy by the axial component of the mean velocity gives the intensity of turbulence, reaching a maximum of 26%.

As said before two setups were used in combination with a 2D LDA system. As a consequence a three dimensional analysis of the flow field can be done for distinctive points in the measurement volume of the combustor. The results are shown in the x-y-plane in Fig. 9. The absolute velocity in the x-y-plane $\sqrt{\overline{u^2} + \overline{v^2}}$ was computed by using measurements from setup B. The out of plane velocity component \overline{w} was derived from setup A. Thus the colored contour plots of \overline{w} are qualitatively the same as shown in Fig. 7 but with different color axis.

Furthermore the measurable area in setup B is smaller than in setup A (compare Fig. 37 and Fig. 9), so that the effective vector plot of absolute velocity in Fig. 9 is smaller than the colored contour plot representing the out of plane velocity. However by using the available data an expansion of the jet can clearly be seen. At $x/D = -1$ it is computed with 10 degrees to the center axis (labeled with 1 in Fig. 9).

In region 2 the axial component is dominating the flow direction. At the center of the combustor (area 3) the flow is decelerated to quasi zero. Velocities below a certain threshold (given by the manufacturer) or even a back flow should be avoided to prevent flashback into the injection modules.

The flow field behind $x/D = -2$ seems to be very turbulent because no direction of flow is dominant.

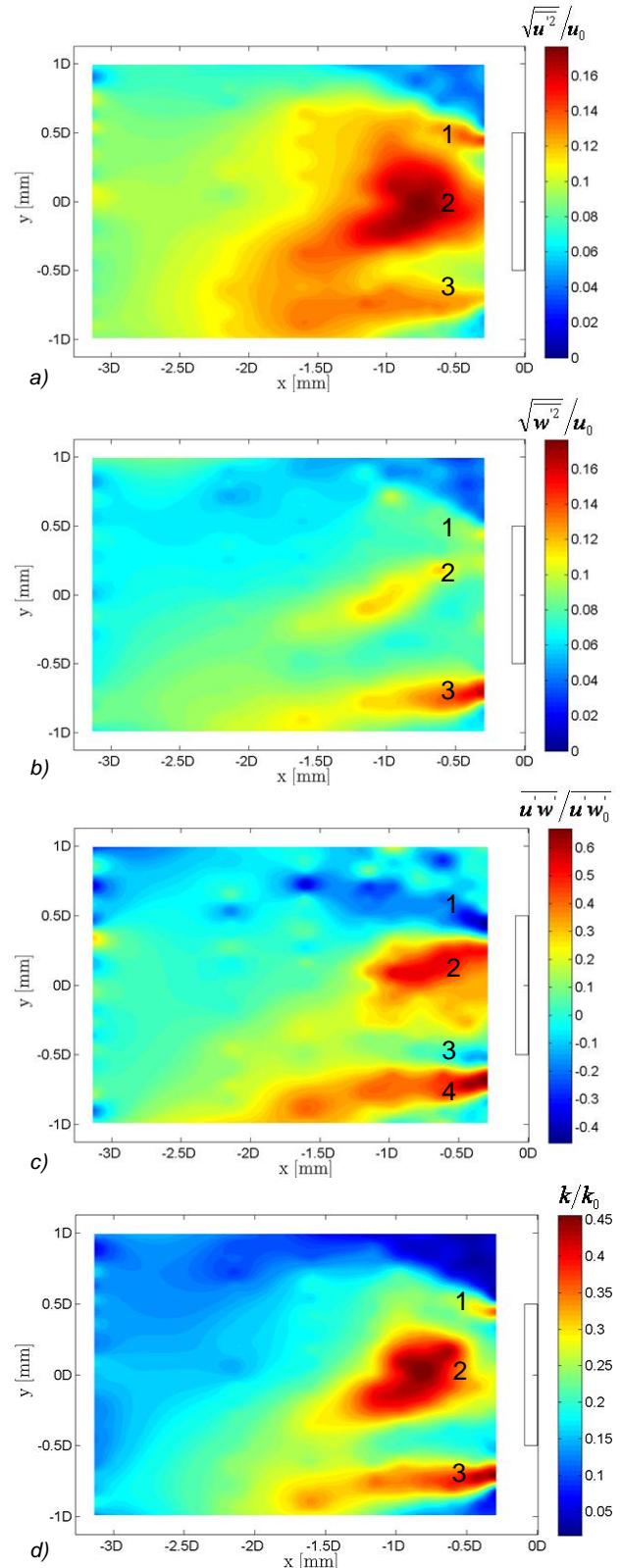


Fig. 8 Colored contour plots of the distribution of a) axial RMS value $\sqrt{u'^2}$, b) tangential RMS value $\sqrt{w'^2}$, c) shear stress $\overline{u'w'}$ and d) turbulent kinetic energy k_e

The calculation of the swirl number is given in Eq. 7 and is an indicator of a reverse flow in a swirling jet. If the swirl number exceeds a value of 0.4 the flow on the center axis begins to stream backwards and forms a recirculation zone [6]. Overall eight swirl numbers, at distance $x/D = -1$ downstream the injectors were computed in the x - y - and x - z -measurement plane. A mean of these eight values results in an averaged swirl number of $S = 0.32$. This calculation confirms the results of the vector plot that no flow is recirculated in the primary combustion zone.

CONCLUSION AND OUTLOOK

A set of LDA-measurements were performed to characterize the aerodynamics in the primary zone of a Low- NO_x -combustor at ambient conditions. By using two different experimental setups, three dimensional information of the flow field in the combustor could be gathered. Measurements were performed in three different planes per LPP-module. The results of the Laser-Doppler-Anemometry are in accordance with the information which can be found in the literature about the technology of LPP-combustion, meaning that no recirculation zone was found and the mean swirl number of $S = 0.32$ is also lower than the characteristically critical swirl number of 0.4. Forming a recirculation zone should be avoided because of the danger of flashback for this type of injector.

Furthermore an asymmetry of the flow in the x - z -plane was found.

The analysis of the flow field also showed the presence of two main vortices (one at each LPP-module) and a smaller vortex between the two burners (Fig. 7 areas 2a and 2b). All three vortices rotate in the same direction, clock wise when looking upstream (Fig. 10). This phenomenon can also be seen in the y - z -plane which is located at a distance of $x/D = -1$ to the front wall of the combustor but is not part of the result presented.

In addition a widening of the jet of approximately 10 degrees at the exit of the LPP-modules was computed.

As the test sector is designed for operation at reactive conditions at elevated pressures and temperatures further research especially in terms of combustion stability will be performed in the future at the Institute for Thermal Turbomachinery and Machine Dynamics (TTM) at Graz

University of Technology. The robustness of the combustion is investigated at steady-state operating condition as well as when being perturbed by a modulation on the air or on the fuel supply. For forced excitation of the air flow the reader is referred to [7] for a detailed description of the new type of flow exciter used.

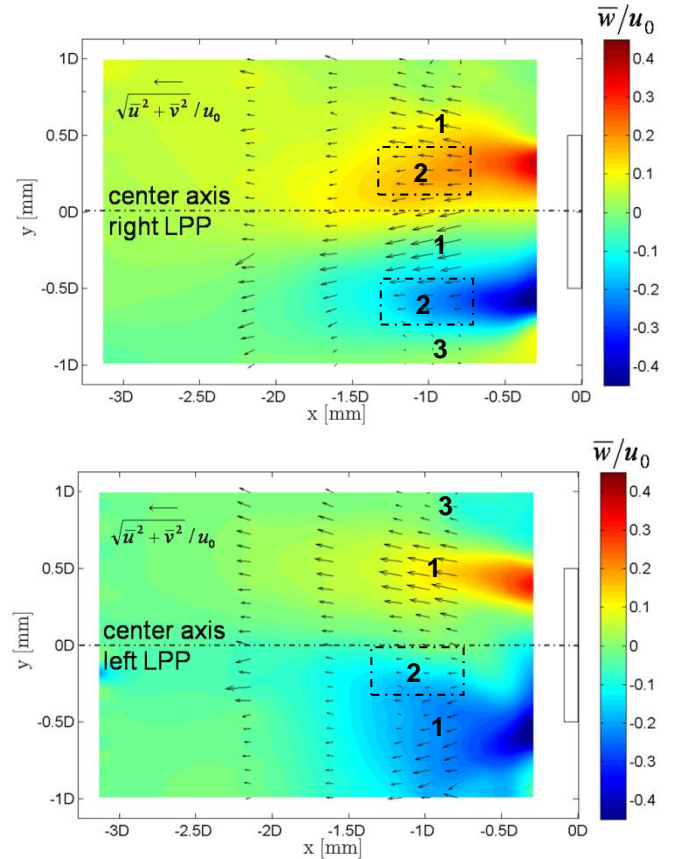


Fig. 9 Velocity plot of LDA-measurement by combining measurements of setup A and B (3D flow field); top: right LPP-module, bottom: left LPP-module

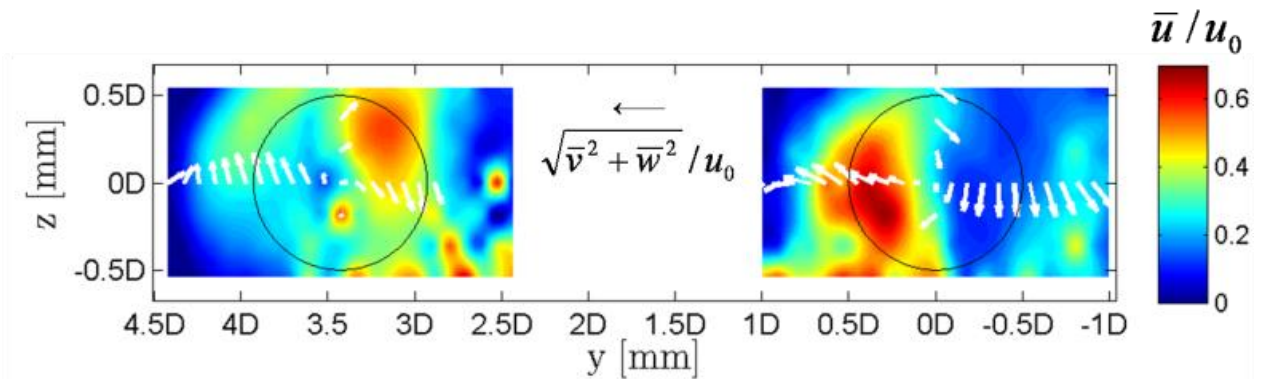


Fig. 10: Velocity plot from LDA-measurement with setup B in the y-z-plane at $x/D = -1$, when looking against the flow direction

NOMENCLATURE

NEWAC	New Aero Engine Core Concepts
TTM	Institute for Thermal Turbomachinery and Machine Dynamics of Graz University of Technology
TU Graz	Graz University of Technology
LPP	Lean Premixed Prevaporized
IRA	Intercooled Recuperative Aero engine
OPR	Overall Pressure Ratio
LDA	Laser Doppler Anemometry
S	Swirl number
RMS	Root mean square

ACKNOWLEDGMENTS

The test rig at TU Graz was supported by the European Commission as part of the Integrated Project "New Aero Engine Core Concepts" (NEWAC, AIP5-CT-2006-030876), which is gratefully acknowledged.

REFERENCES

- [1] Wilfert G., Sieber J., Rolt A., Baker N., Touyeras A., Colantuoni S., "New Environmental Friendly Aero Engine Core Concepts", ISABE-2007-1120, 2007
- [2] Bock S., Horn W., Wilfert G., Sieber J., "Active Technology within the NEWAC Research Program for cleaner and more efficient Aero engines", CEAS-2007-1235, 2007
- [3] Joos F., "Technische Verbrennung", 1. Auflage, Springer, 2006
- [4] Ruck B., „Lasermethoden in der Strömungsmess-technik“, 1.Auflage, AT-Fachverlag GmbH Stuttgart, 1990
- [5] Beer J.M., Chigier N.H., "Combustion Aerodynamics", Applied Science, London, 1972
- [6] Lefebvre A.H., "Gas Turbine Combustion", 2nd Edition, Taylor & Francis Group New York, 1999
- [7] Giuliani F., Lang A., Gradl K., Siebenhofer P., "Flow modulation for refined control of the combustion dynamics using a novel actuator", ASME Conf. Proc. 2011, GT-2011-4507
- [8] Lang A, Unsteady Combustion Phenomena in Current and Future Aero Engines, Phd Thesis, Graz, 2011